

## ORIGINAL ARTICLE

# Protein nanogelation using vitamin B<sub>6</sub>-bearing pullulan: effect of zinc ions

Yuji Tsuchido<sup>1,4</sup>, Yoshihiro Sasaki<sup>1,2</sup>, Shin-ichi Sawada<sup>2,3</sup> and Kazunari Akiyoshi<sup>1,2,3</sup>

Nanogels are nanometer-sized hydrogel nanoparticles with three-dimensional networks of crosslinked polymer chains. We have previously reported a method for constructing protein nanogels using vitamin B<sub>6</sub> (pyridoxal)-bearing pullulan (PLPP) as a bio-crosslinker. To validate the potential for using this bio-crosslinker to prepare protein nanogels, we developed an improved method using metal ions to enhance the affinity between the protein and the bio-crosslinker. We investigated the binding of PLPP as a bio-crosslinker to a protein to produce protein nanogels using anionic bovine serum albumin (BSA) as a model protein. Ultraviolet-visible spectroscopic titration of PLPP with BSA showed that the binding of the PLPP to the BSA via the formation of Schiff bases was significantly enhanced in the presence of zinc ions because of the coordination of the Schiff base to metal ions, which shifted the equilibrium of the reaction to the Schiff base formation side. Dynamic light scattering measurements, high-performance liquid chromatography and transmission electron microscopy confirmed that the zinc ions enhanced the ability of PLPP to form nanogels by crosslinking with the anionic BSA despite the strong electrostatic repulsion between the two molecules.

*Polymer Journal* (2015) 47, 201–205; doi:10.1038/pj.2014.120; published online 17 December 2014

## INTRODUCTION

Nanogels are nanosized hydrogel particles with three-dimensional crosslinked networks of hydrophilic polymers (<100 nm).<sup>1–4</sup> In recent years, nanogels have attracted growing interest for their potential biomedical applications because of their small particle sizes and hydrogel-like characteristics, especially high water uptake, high mechanical stability and high loading capacity for bioactive compounds, such as drugs, proteins and DNA/RNA. Because of their small size, nanogels rapidly respond to microenvironmental factors, such as temperature and pH, whereas larger macrogels take longer, often up to a few days, to respond to such factors. These properties of nanogels are particularly useful in the controlled release of bioactive compounds.

We have developed self-assembled nanogels composed of hydrophobic polysaccharides, such as cholesterol-bearing pullulan (CHP).<sup>1,2</sup> CHP forms a stable amphiphilic nanogel in water by the self-association of the hydrophobic groups, forming physical crosslinks between individual molecules. CHP nanogels can trap proteins and display molecular chaperone-like activity.<sup>3</sup> CHP nanogels are also useful for protein delivery, such as cancer vaccines and cytokine therapy.<sup>6,7</sup> Several methods, in addition to hydrophobic interaction, can be used to generate crosslinks including electrostatic interactions<sup>8</sup> and host–guest interactions with cyclodextrin.<sup>9</sup> Nanogels, which were developed by exploiting a wide range of intermolecular forces, show great potential for the preparation of novel stimulus-responsive nanomaterials, including photoresponsive<sup>10</sup> and pH-responsive

nanogels.<sup>11</sup> Several biomolecules, including oligopeptides,<sup>12,13</sup> proteins,<sup>14</sup> antibodies<sup>15</sup> and oligonucleotides,<sup>16</sup> have also been used as crosslinkers to prepare macroscale hydrogels other than nanogels. One of the main advantages of bio-crosslinked hydrogels is that their responses to stimuli are controlled and modulated by the biomolecule used as the crosslinker.<sup>17</sup>

We previously reported a new method for preparing protein nanogels using vitamin B<sub>6</sub> (pyridoxal)-bearing pullulan (PLPP) as a bio-crosslinker (Figure 1).<sup>18</sup> Vitamin B<sub>6</sub> is a coenzyme for vitamin B<sub>6</sub>-dependent enzymes.<sup>19</sup> One of the important chemical characteristics of vitamin B<sub>6</sub> is that it forms a Schiff base with the aldehyde group of pyridoxal and the amino group of biomolecules such as oligopeptides, oligonucleotides or proteins in an aqueous solution at physiological pH. Using vitamin B<sub>6</sub> as the bio-crosslinker, nanogels were prepared via the formation of a Schiff base between the pyridoxal groups and the protein's amino groups. The Schiff base is considered to be a dynamic covalent bond that is regulated by environmental factors, such as pH. Therefore, the pH dependence of the formation of the Schiff base was exploited to construct a pH-sensitive nanogel system. These pH-sensitive hybrid nanogels, which comprise a variety of biomolecules, are potentially useful as nanocarriers in drug delivery systems. For example, acid-sensitive protein nanogels could be used for cytosolic protein delivery.

Despite these advantages, nanogel formation using a bio-crosslinker has a limitation in that anionic bio-crosslinkers cannot be used with

<sup>1</sup>Institute of Biomaterials and Bioengineering, Tokyo Medical and Dental University, Tokyo, Japan; <sup>2</sup>Department of Polymer Chemistry, Graduate School of Engineering, Kyoto University, Kyoto, Japan and <sup>3</sup>The Exploratory Research for Advanced Technology (ERATO), Japan Science and Technology Agency (JST), Tokyo, Japan

<sup>4</sup>Current address: Department of Materials and Life Sciences, Faculty of Science and Technology, Sophia University, 7-1 Kioi-cho, Chiyoda-ku, Tokyo 102-8554, Japan

Correspondence: Professor K Akiyoshi, Department of Polymer Chemistry, Graduate School of Engineering, Kyoto University, Katsura, Nishikyo-ku, Kyoto 615-8510, Japan. E-mail: akiyoshi@bio.polym.kyoto-u.ac.jp

Received 29 July 2014; revised 15 October 2014; accepted 21 October 2014; published online 17 December 2014

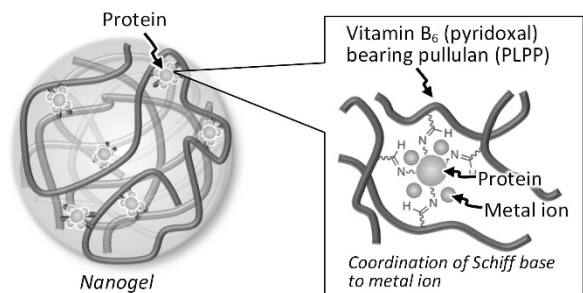


**Figure 1** Schematic representation of a protein-bio-crosslinker nanogel formed via Schiff bases.

acidic (anionic) proteins because of the strong electrostatic repulsions between the molecules. Because the majority of water-soluble proteins are acidic or neutral at physiological pH, it is necessary to develop a method to use bio-crosslinkers with acidic proteins. Accordingly, to validate the general applicability of using bio-crosslinkers to prepare nanogels, we developed an improved method using metal ions to enhance the affinity between proteins and the bio-crosslinker.

## MATERIALS AND METHODS

### Materials

PLPP (Figure 2) with an average molecular weight ( $M_w$ ) of  $1.0 \times 10^5$  (3.8 pyridoxal phosphate groups per 100 glycoside units) was synthesized as previously reported.<sup>18</sup> 2-[4-(2-hydroxyethyl)-1-piperazinyl]-ethanesulfonic acid (HEPES2-[4-(2-hydroxyethyl)-1-piperazinyl]-ethanesulfonic acid) and bovine albumin (lyophilized) were purchased from Nacalai Tesque, Inc. (Kyoto, Japan). Sodium chloride, sodium hydroxide, hydrochloric acid and zinc chloride were purchased from Wako Pure Chemical Industries, Ltd (Osaka, Japan). All chemicals were of the highest commercially available grade and were used without further purification.

### Preparation of nanogels using a bio-crosslinker

The PLPP was dissolved in buffer (100 mM HEPES, 100 mM NaCl, pH 7.0) by stirring for 1 h at 25 °C. The suspension was then sonicated with a probe-type sonicator (SONIFIER 250; Branson Ultrasonics Co., Danbury, CT, USA; tip diameter, 2 mm) at 20 W for 15 min on ice and was filtered through a poly(vinylidene fluoride) membrane filter (MILLEX GV; Millipore Co. Ltd, MA, USA; pore size, 0.22  $\mu\text{m}$ ) to remove dust or metallic particles shed from the titanium transducer tip. The clear aqueous PLPP solution was mixed with the protein solution and the zinc chloride solution, and the mixture was incubated at 25 °C for 1 h to yield the PLPP–bovine serum albumin (BSA) complex.

### Ultraviolet-visible spectral analysis

The formation of Schiff bases between the PLPP and the BSA was evaluated by ultraviolet-visible spectral measurements using a HITACHI U-3900H spectrophotometer (Hitachi High-Technologies Co. Ltd, Tokyo, Japan). PLPP was dissolved in buffer (100 mM HEPES, 100 mM NaCl, pH 7.0) by stirring for 1 h at 25 °C, and the PLPP solution (0.05 mM; molar concentration of PLP embedded in pullulan) was prepared as described above. The ultraviolet-visible spectra of PLPP were measured at 25 °C after adding the BSA in the presence or absence of zinc ions.

### Size exclusion chromatography

PLPP–protein binding was evaluated by size exclusion chromatography, which consisted of a CCPS dual pump, a CO-8020 column oven, a RI-8020 refractive index detector and a UV-8020 UV detector (Tosoh Co. Ltd, Tokyo, Japan). All measurements were performed using a Superdex 75 10/300 GL column with a guard column (GE Healthcare Japan, Tokyo, Japan). Samples were eluted with 100 mM HEPES/100 mM NaCl buffer (pH 7.0) at a flow rate of 0.5 ml  $\text{min}^{-1}$  at 25 °C. Sample elution was monitored by an UV detector at 280 nm.

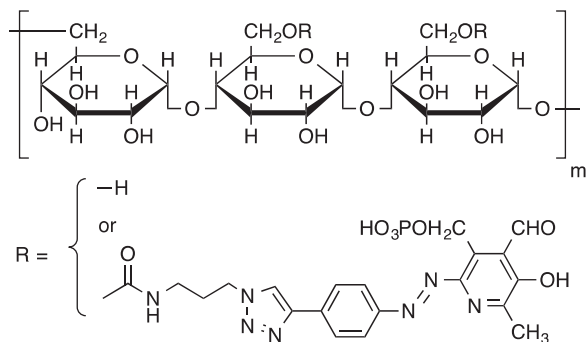


**Figure 2** Chemical structure of PLPP.

### Dynamic light scattering (DLS)

DLS measurements were carried out at 25 °C using a Zetasizer Nano ZS (Malvern Instruments Ltd, Malvern, Worcestershire, UK) at a wavelength of 633 nm and a detection angle of 173° to determine the sizes of the PLPP–BSA nanogels. Optically clear sample solutions were obtained by ultrasonication at 20 W for 15 min on ice and filtration through a poly(vinylidene fluoride) membrane filter (MILLEX GV; Millipore Co. Ltd; pore size, 0.22  $\mu\text{m}$ ) to remove any dust in the solution. The concentration of the sample was kept constant at 1.0 mg  $\text{ml}^{-1}$ . The measured autocorrelation function was analyzed via a cumulant method, and the hydrodynamic diameter ( $D_{\text{hy}}$ ) was determined using the Stokes–Einstein equation.<sup>20</sup>

### Native agarose gel electrophoresis

Complexation between the PLPP and the BSA in the presence of zinc ions was evaluated using native agarose gel electrophoresis under non-denaturing conditions. The samples were run on a 6% homogenous gel using a Bio-Rad protein electrophoresis unit (Bio-Rad Laboratories, Hercules, CA, USA). The running buffer was 0.5× Tris/borate/ethylene-diaminetetraacetic acid buffer (pH 8.0). The gels were then stained with Coomassie blue for analysis.

### Transmission electron microscopy (TEM)

TEM was used to assess the formation of the nanogels with PLPP. First, 20  $\mu\text{l}$  of the PLPP–BSA nanogels in the presence of zinc ions was placed on a 200-mesh copper grid deposited with carbon. The grid was dried under vacuum and was washed with a small amount of water. TEM observations were performed using a Hitachi H-7100 (Hitachi Ltd, Tokyo, Japan).

## RESULTS AND DISCUSSION

### Formation of Schiff bases between the bio-crosslinker and BSA

The binding behavior of the PLPP as a bio-crosslinker to an anionic protein, in this case BSA, was examined using electronic absorption spectroscopy at 25 °C. BSA has a molecular weight of 66 800 Da and an isoelectric point of 4.9 and is composed of 585 amino-acid residues (60 lysine residues) with no disulfide bridges. The maximum absorption of PLPP dissolved in water at pH 7.0 was at 481 nm. Adding BSA to the PLPP solution did not change the absorption spectra (Figure 3a). This result indicates that the apparent binding affinity between PLPP and BSA is very low because of the strong electrostatic repulsion between the anionic BSA and the anionic PLPP. To increase the apparent binding affinity between the molecules, metal ions were added to the PLPP and BSA solution. Some metal ions, including copper and zinc, enhance the formation of Schiff bases because the coordination of the Schiff base to the metal ions shifts the equilibrium of the reaction to the Schiff base formation side.<sup>21</sup> Accordingly, zinc ions changed the UV spectra of the BSA and PLPP solution, which is consistent with the formation of Schiff bases between the amino groups of the BSA and the formyl groups of the pyridoxal moieties in

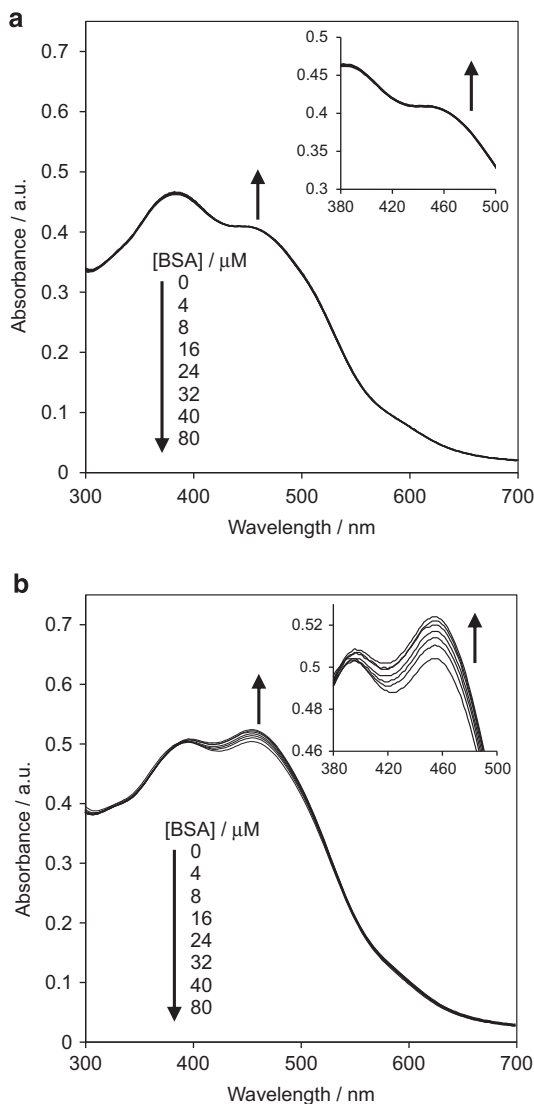


**Figure 3** Change in the UV spectra of PLPP (0.2 mM, as the molar concentration of PLP embedded in pullulan) following the addition of BSA in the absence (a) or presence (b) of 0.5 mM zinc ion. HEPES: 100 mM; NaCl: 100 mM.

PLPP (Figure 3b). UV titration of PLPP and BSA in the presence of zinc ions confirmed the formation of Schiff bases with an apparent binding constant of  $4.7 \times 10^5 \text{ M}^{-1}$ , whereas the binding constant in the absence of zinc ions was  $< 10^3 \text{ M}^{-1}$  (Figure 4). These results indicate that Schiff base formation was significantly increased by the coordination of the zinc ions.

#### Nanogel formation by complexation of BSA with the bio-crosslinker

Complexation of PLPP and BSA was evaluated by native agarose gel electrophoresis. Figure 5 shows the agarose electrophoresis analysis of free BSA and the mixture of the BSA and PLPP in the presence of zinc ions. In Lane 3, the BSA migrated toward the positive electrode because of its negative charge. When PLPP was added to the BSA solution in the presence of zinc ions, the band corresponding to the free BSA was absent, and a band corresponding to the PLPP–BSA complex was detected (Lane 2). Notably, no band was detected for the

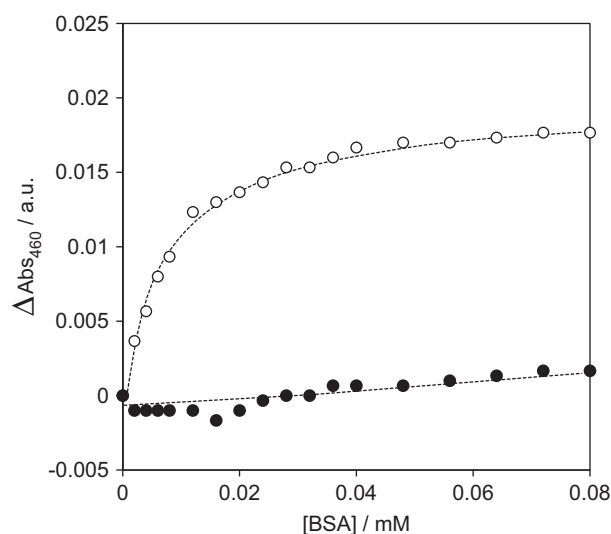


**Figure 4** Changes in absorbance at 460 nm following BSA titration of PLPP at 25 °C in 100 mM HEPES buffer containing 100 mM NaCl at pH 7.0 in the presence (open circle) or absence (closed circle) of zinc ions.

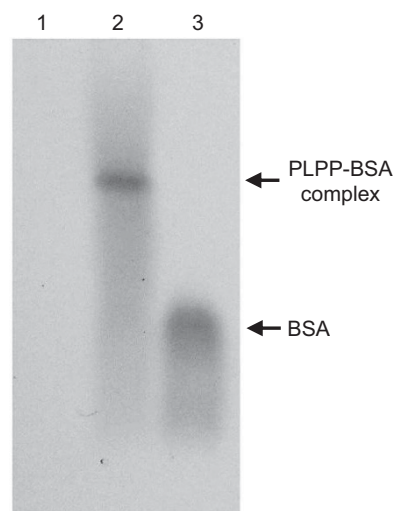


**Figure 5** Native agarose gel electrophoresis of the complexation of PLPP with BSA after 24 h incubation at 25 °C. Lane 1, PLPP; lane 2, PLPP and BSA; lane 3, BSA. PLPP: 0.18 mM (molar concentration of PLP embedded in pullulan); BSA: 0.27 mM (molar concentration of lysine residues in protein); HEPES: 100 mM; NaCl: 100 mM;  $\text{ZnCl}_2$ : 2.0 mM.

PLPP alone (Lane 1). These results indicate that the negative charge of the BSA was decreased by complexation with the PLPP in the presence of zinc ions.

The complexation of PLPP and BSA was also evaluated using size exclusion chromatography. The chromatograms of the PLPP, the free BSA, and the mixture of PLPP and BSA in the presence or absence of zinc ions are shown in Figure 6. A peak corresponding to free BSA was observed at an elution time of 20 min with absorption at 280 nm. In the absence of zinc ions, even after mixing PLPP and BSA for 1 h, the peaks corresponding to the PLPP and the free BSA were unchanged, which indicates no complexation between the PLPP and the BSA in the current conditions (Figure 6a). This lack of complexation is due to

the very low binding affinity of PLPP with BSA, as observed in the UV spectra described above. When PLPP was mixed with BSA in the presence of zinc ions for 1 h, the peak corresponding to free BSA disappeared and the size of the peak corresponding to PLPP increased (Figure 6b). These results indicate that a significant amount of BSA interacts with PLPP, and we estimated that almost 100% of the BSA present in the solution formed complexes with PLPP.

#### Characterization of the BSA nanogel

The size exclusion chromatography results indicated that the BSA–PLPP complex was much larger than free BSA. These results suggest that BSA, which has multiple binding sites, bound to the polysaccharide by the formation of Schiff bases, which yielded larger nanogels. To confirm that the nanogels were formed by the complexation between the PLPP and the BSA, we performed DLS measurements (Table 1). Unfortunately, the hydrodynamic diameter ( $D_{hy}$ ) of the PLPP aqueous

solution and the free BSA solution could not be determined using DLS because of the low light-scattering intensity of these solutions. These findings suggest that the PLPP and the BSA were molecularly dispersed in the water and did not associate with macromolecules under these conditions. In the presence of zinc ions, the  $D_{hy}$  of the PLPP and the BSA solutions increased significantly with an increase in the BSA concentration, which is consistent with the formation of nanogels, even though the size distribution of the current nanogels was larger than that of conventional CHP nanogels.<sup>5</sup> One of the possible explanations for the  $D_{hy}$  increase is that the number of crosslinking points per BSA molecule decreased with an increase in the BSA concentration so that the amount of BSA involved the nanogel increased, resulting in the formation of large particles. In the absence of zinc ions, the light scattering of the PLPP and the BSA solution was unmeasurable.

**Table 1** Hydrodynamic diameters ( $D_{hy}$ ) of PLPP and BSA determined by dynamic light-scattering measurements in the presence and absence of zinc ions at 25 °C.

Sample			$D_{hy}/nm$ (PDI) <sup>a</sup>
[PLPP] /mM <sup>b</sup>	[BSA] /mM <sup>c</sup>	[Zn <sup>2+</sup> ] /mM	
0.2	0	2	ND <sup>d</sup>
0.2	0.1	2	39.0 (0.4)
0.2	0.2	2	39.3 (0.5)
0.2	0.3	2	129 (0.4)
0.2	0.4	2	203 (0.7)
0.2	0	0	ND <sup>d</sup>
0.2	0.4	0	ND <sup>d</sup>
0	0.4	2	ND <sup>d</sup>

Abbreviations: BSA, bovine serum albumin; PDI, polydispersity index, PLPP, pyridoxal-bearing pullulan; ND, not determined.

<sup>a</sup>The polydispersity indices (PDIs) indicating the size distribution of the particle are given in parentheses.

<sup>b</sup>The molar concentration of PLP in PLPP.

<sup>c</sup>The molar concentration of lysine residues in BSA.

<sup>d</sup>Not determined; the  $D_{hy}$  could not be determined because of the low light-scattering intensity of the solution.

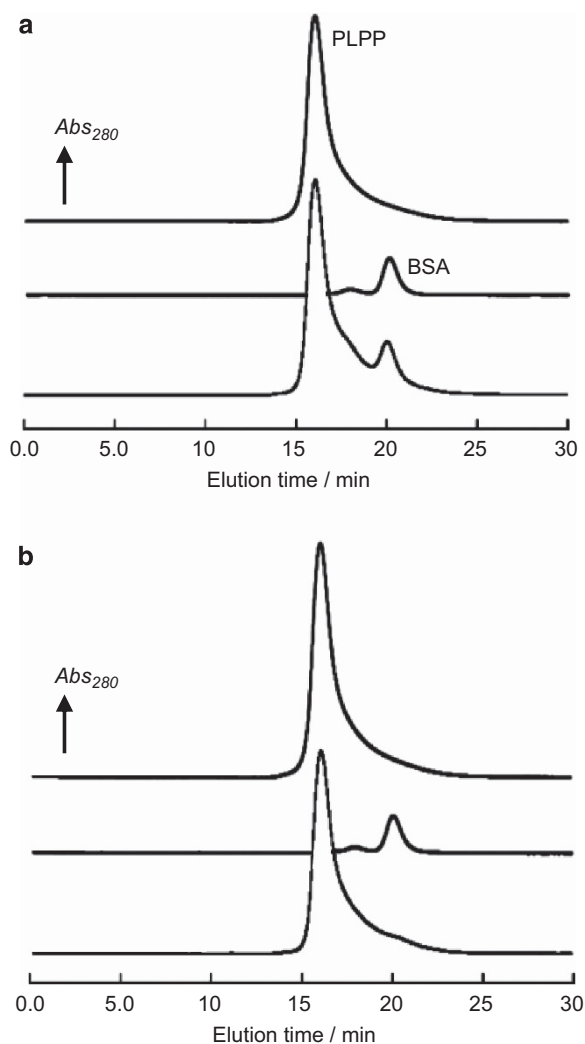


**Figure 6** Elution profiles (280 nm) of PLPP (top; 0.2 mM, molar concentration of PLP embedded in pullulan), BSA (middle; 0.2 mM, as a concentration of lysine residue in BSA) and a mixture of PLPP and BSA (bottom) in the absence (a) or presence (b) of zinc ions (2.0 mM). All measurements were performed on an SEC system (Tosoh, Tokyo, Japan) and a Superdex 75 10/300 GL column (GE Healthcare) using 100 mM HEPES/100 mM NaCl (pH 7.0) as the elution buffer at 25 °C. The flow rate was 0.5 ml min<sup>-1</sup>.

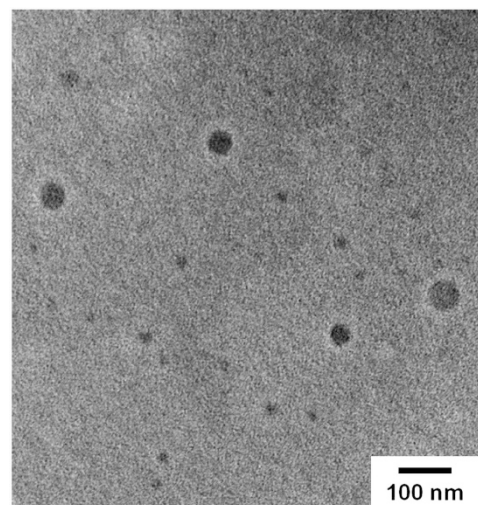


**Figure 7** TEM images of the PLPP–BSA nanogel at pH 7.0. PLP: 0.2 mM (molar concentration of PLP embedded in pullulan); BSA: 0.1 mM (concentration of lysine residue in BSA); ZnCl<sub>2</sub>: 2.0 mM; NaCl: 100 mM; HEPES: 100 mM.

The formation of nanogels was also analyzed using TEM (Figure 7). The TEM images indicated the formation of spherical nanogels even in the absence of a staining reagent. This is likely due to the existence of zinc ions within nanogels that formed owing to the complexation between PLPP and BSA. The size of the nanogel was consistent with the  $D_{hy}$  determined by DLS. Although the reason for the formation of a nanogel rather than a macrogel is not fully clear; the polysaccharide chain of PLPP may coat the protein and stop further aggregation.

## CONCLUSION

The use of PLPP as a bio-crosslinker yielded protein nanogels by forming Schiff bases between the pyridoxal moiety of the PLPP and the protein's amino groups in the presence of zinc ions. By coordinating the Schiff base with zinc ions, the apparent binding constant between PLPP and BSA was drastically increased. The formation of hybrid nanogels via coordinated complexation of Schiff bases and zinc ions is a promising strategy for preparing nanogels of biomedically useful anionic proteins. For example, nanogels containing anionic proteins could be used for cytosolic protein delivery. These biomedical applications are under investigation in our laboratory.

## ACKNOWLEDGEMENTS

This work was supported by Grants-in-Aid for Scientific Research (No. 23107510) in the Innovative Area 'Fusion Materials' (Area No. 2206) from the Ministry of Education, Culture, Sports, Science and Technology (MEXT).

- 1 Sasaki, Y. & Akiyoshi, K. Nanogel engineering for new nanobiomaterials: from chaperoning engineering to biomedical applications. *Chem. Rec.* **10**, 366–376 (2010).
- 2 Sasaki, Y. & Akiyoshi, K. Self-assembled nanogel engineering for advanced biomedical technology. *Chem. Lett.* **41**, 202–208 (2012).
- 3 Oh, J. K., Drumright, R., Siegwart, D. J. & Matyjaszewski, K. The development of microgels/nanogels for drug delivery applications. *Prog. Polym. Sci.* **33**, 448–477 (2008).
- 4 Reamdonck, K., Demeester, J. & De Smedt, S. Advanced nanogel engineering for drug delivery. *Soft Matter* **5**, 707–715 (2009).
- 5 Sasaki, Y. & Akiyoshi, K. Development of an artificial chaperone system based on cyclodextrin. *Curr. Pharm. Biotechnol.* **11**, 300–305 (2010).
- 6 Nochi, T., Yuki, Y., Takahashi, H., Sawada, S., Mejima, M., Kohda, T., Harada, N., Kong, I. G., Sato, A., Kataoka, N., Tokuhara, D., Kurokawa, S., Takahashi, Y., Tsukada, H., Kozaki, S., Akiyoshi, K. & Kiyono, H. Nanogel antigenic protein-delivery system for adjuvant-free intranasal vaccines. *Nat. Mater.* **9**, 572 (2010).
- 7 Hasegawa, U., Sawada, S., Shimizu, T., Kishida, T., Otsuji, E., Mazda, O. & Akiyoshi, K. Raspberry-like assembly of cross-linked nanogels for protein delivery. *J. Control. Release* **140**, 312–317 (2009).
- 8 Shu, S., Zhang, X., Teng, D., Wang, Z. & Li, C. Polyelectrolyte nanoparticles based on water-soluble chitosan-poly(L-aspartic acid)-polyethylene glycol for controlled protein release. *Carbohydr. Res.* **344**, 1197–1204 (2009).
- 9 Daoud-Mahammed, S., Couvreur, P., Bouchemal, K., Chéron, M., Lebas, G., Amiel, C. & Gref, R. Cyclodextrin and polysaccharide-based nanogels: entrapment of two hydrophobic molecules, benzophenone and tamoxifen. *Biomacromolecules* **10**, 547–554 (2009).
- 10 Hirakura, T., Nomura, Y., Aoyama, Y. & Akiyoshi, K. Photoresponsive nanogels formed by the self-assembly of spiropyran-bearing pullulan that act as artificial molecular chaperones. *Biomacromolecules* **5**, 1804–1809 (2004).
- 11 Shen, X., Zhang, L., Jiang, X., Hu, Y. & Guo, J. Reversible surface switching of nanogel triggered by external stimuli. *Angew. Chem. Int. Ed.* **46**, 7104–7107 (2007).
- 12 Šubr, V., Duncan, R. & Kopeček, J. J. Release of macromolecules and daunomycin from hydrophilic gels containing enzymatically degradable bonds. *Biomater. Sci. Polym. Ed.* **1**, 261–278 (1990).
- 13 West, J. L. & Hubbell, J. A. Polymeric biomaterials with degradation sites for proteases involved in cell migration. *Macromolecules* **32**, 241–244 (1999).
- 14 Obaidat, A. A. & Park, K. Characterization of glucose dependent gel-sol phase transition of the polymeric glucose-concanavalin A hydrogel system. *Pharm. Res.* **13**, 989–995 (1996).
- 15 Miyata, T., Asami, N. & Uragami, T. A reversibly antigen-responsive hydrogel. *Nature* **399**, 766–769 (1999).
- 16 Nagahara, S. & Matsuda, T. Hydrogel formation via hybridization of oligonucleotides derivatized in water-soluble vinyl polymers. *Polym. Gels Netw.* **4**, 111–127 (1996).
- 17 Kopeček, J. Hydrogel biomaterials: a smart future? *Biomaterials* **28**, 5185–5192 (2007).
- 18 Sasaki, Y., Tsuchido, Y., Sawada, S. & Akiyoshi, K. Construction of protein-crosslinked nanogels with vitamin B6 bearing polysaccharide. *Polym. Chem.* **2**, 1267–1270 (2011).
- 19 Snell, E. E. & Di Mari, S. J. *The Enzymes* 3rd edn, vol. 2 (eds Snell E. E., Di Mari S. J.) (Academic Press, New York, NY, USA, 1970).
- 20 Koppel, D.E. Analysis of macromolecular polydispersity in intensity correlation spectroscopy: the method of cumulants. *J. Chem. Phys.* **57**, 4814–4820 (1972).
- 21 Matsuo, Y. Pyridoxal catalysis of non-enzymatic transamination in ethanol solution. *J. Am. Chem. Soc.* **79**, 2016–2019 (1957).